Catalytic mechanism of the haloalkane dehalogenase LinB from Sphingomonas paucimobilis UT26

Prokop, Z; Monincova, M; Chaloupkova, R; Klvana, M; Nagata, Y; Janssen, Dick; Damborsky, J; Klvaňa, Martin

Published in:
The Journal of Biological Chemistry

DOI:
10.1074/jbc.M307056200

Publication date:
2003

THE JOURNAL OF BIOLOGICAL CHEMISTRY
Vol. 278, No. 46, Issue of November 14, pp. 45094–45100, 2003
Printed in U.S.A.

Catalytic Mechanism of the Haloalkane Dehalogenase LinB from *Sphingomonas paucimobilis* UT26*

Received for publication, July 2, 2003, and in revised form, August 25, 2003
Published, JBC Papers in Press, September 1, 2003, DOI 10.1074/jbc.M307056200

Zbyněk Prokop‡§, Marta Monincová‡, Radka Chaloupková‡, Martin Klvaňa‡, Yuji Nagata¶, Dick B. Janssen‖, and Jiří Damborský‡

From the ‡National Centre for Biomolecular Research, Masaryk University, Kotlarska 2, 611 37 Brno, Czech Republic, the ¶Department of Life Sciences, Graduate School of Life Sciences, Tohoku University, 2-1-1 Katahira, Sendai, 980-8577, Japan, and the ‖University of Groningen, Nijenborgh 4, 9747 AG Groningen, The Netherlands

Haloalkane dehalogenases are bacterial enzymes capable of carbon-halogen bond cleavage in halogenated compounds. To obtain insights into the mechanism of the haloalkane dehalogenase from *Sphingomonas paucimobilis* UT26 (LinB), we studied the steady-state and presteady-state kinetics of the conversion of the substrates 1-chlorohexane, chlorocyclohexane, and bromocyclohexane. The results lead to a proposal of a minimal kinetic mechanism consisting of three main steps: (i) substrate binding, (ii) cleavage of the carbon-halogen bond with simultaneous formation of an alkyl-enzyme intermediate, and (iii) hydrolysis of the alkyl-enzyme intermediate. Release of both products, halide and alcohol, is a fast process that was not included in the reaction mechanism as a distinct step. Comparison of the kinetic mechanism of LinB with that of haloalkane dehalogenase DhlA from *Xantobacter autotrophicus* GJ10 and the haloalkane dehalogenase DhaA from *Rhodococcus rhodochrous* NCIMB 13064 shows that the overall mechanisms are similar. The main difference is in the rate-limiting step, which is hydrolysis of the alkyl-enzyme intermediate in LinB, halide release in DhlA, and liberation of an alcohol in DhaA. The occurrence of different rate-limiting steps for three enzymes that belong to the same protein family indicates that extrapolation of this important catalytic property from one enzyme to another can be misleading even for evolutionary closely related proteins. The differences in the rate-limiting step were related to: (i) number and size of the entrance tunnels, (ii) protein flexibility, and (iii) composition of the halide-stabilizing active site residues based on comparison of protein structures.

Haloalkane dehalogenases (EC 3.8.1.5) make up an important class of enzymes that are able to cleave carbon-halogen bonds in halogenated aliphatic compounds. There is a growing interest in these enzymes because of their potential use in bioremediation, as industrial biocatalysts, or as biosensors. Structurally, haloalkane dehalogenases belong to the α/β-hydrolase fold superfamily (1). Without exception, haloalkane dehalogenases contain a nucleophile elbow (2), which is the most conserved structural feature within the α/β-hydrolase fold. The other highly conserved region in haloalkane dehalogenases is the central β-sheet. Its strands, flanked on both sides by α-helices, form the hydrophobic core of the main domain that carries the catalytic triad Asp-His-(Asp/Glu). The second domain, consisting solely of α-helices, lies like a cap on top of the main domain. Residues at the interface of the two domains form the active site. Whereas there is significant similarity in the catalytic core, the sequence and structure of the cap domain diverge considerably among different dehalogenase. The cap domain is proposed to play a prominent role in determining substrate specificity (3, 4). A reaction mechanism for haloalkane dehalogenase has been proposed on the basis of x-ray crystallographic (5), site-directed mutagenesis (6, 7), and kinetic (8, 9) studies with the haloalkane dehalogenase of *Xantobacter autotrophicus* GJ10 (DhlA). Catalysis proceeds by the nucleophilic attack of the carboxylate oxygen of an aspartate group on the carbon atom of the substrate, yielding displacement of the halogen as halide and formation of a covalent alkyl-enzyme intermediate. The alkyl-enzyme intermediate is subsequently hydrolyzed by a water molecule that is activated by a histidine. A catalytic acid (Asp or Glu) stabilizes the charge developed on the imidazole ring of the histidine during the hydrolytic half-reaction.

A number of haloalkane dehalogenases from different bacteria have been purified and biochemically characterized. A principal component analysis of activity data indicated the presence of three specificity classes within this family of enzymes (10, 11). Three haloalkane dehalogenases representing these different classes have been isolated and characterized in detail so far: the haloalkane dehalogenase DhlA (12), the haloalkane dehalogenase LinB from *Sphingomonas paucimobilis* UT26 (11) and the haloalkane dehalogenase DhaA from *Rhodococcus rhodochrous* NCIMB 13064 (13). The kinetic mechanism has been solved for DhlA (9) and DhaA (14). Comparison of the kinetic mechanism of DhlA and DhaA shows that the overall scheme is similar. The main difference was found at rate-limiting steps. For their best substrates, it was found that the rate of halide release represents the slowest step in the catalytic cycle of DhlA, whereas liberation of the alcohol is rate-limiting in the catalytic action of DhaA.

This study presents detailed insight into the kinetic mechanism of the haloalkane-dehalogenase LinB that is obtained using steady-state as well as presteady-state kinetic techniques. The similarities and differences between the kinetics of the three well studied haloalkane dehalogenases are also discussed in this report.

MATERIALS AND METHODS

Protein Expression and Purification—To overproduce His-tagged LinB enzyme, the plasmid pMLBH6 (15) was used. *Escherichia coli*

* This work was supported by Grant LN00A016 from the Czech Ministry of Education. The costs of publication of this article were defrayed in part by the payment of page charges. This article must therefore be hereby marked "*advertisement*" in accordance with 18 U.S.C. Section 1734 solely to indicate this fact.

§ Recipient of a scholarship from the Federation of European Microbiological Societies. To whom correspondence should be addressed. Fax: 420-5-41129506; E-mail: zbynek@chemi.muni.cz.

BL21 (DE3) harboring pMLBH6 was cultured in 0.25 liters of Luria broth at 37 °C. Induction of dehalogenase synthesis was initiated by addition of isopropyl-β-D-thiogalactopyranoside to a final concentration of 0.5 mM when the culture reached an optical density of 0.6 at 600 nm. After induction, the culture was incubated at 30 °C for 4 h and then harvested. The cells were disrupted by sonication using a Soniprep 150 (Sanyo). A cell-free extract was obtained by centrifugation at 100,000 × *g* for 1 h. The dehalogenase was purified on a Ni-nitrilotriacetic acid Sepharose column HR 16/10 (Qiagen). The His-tagged LinB (16) was bound to the resin in the equilibrating buffer, which contained 20 mM potassium phosphate buffer pH 7.5, 0.5 M sodium chloride and 10 mM imidazole. Unbound and weakly bound proteins were washed with buffer containing 60 mM imidazole. The His-tagged enzyme was then eluted with buffer with 160 mM imidazole. The active fractions were pooled and dialyzed overnight against 50 mM potassium phosphate buffer, pH 7.5. The enzyme was stored at 4 °C in 50 mM potassium phosphate buffer, pH 7.5, containing 10% glycerol and 1 mM 2-mercaptoethanol. The enzyme was dialyzed overnight at 4 °C against 0.13 mM glycine buffer, pH 8.6, for stopped flow and rapid quench flow experiments.

Steady-State Kinetics—Dehalogenation reactions were performed at 37 °C in 25-ml Reacti-Flasks closed by Mininert Valves. Nine different concentrations of substrate in glycine buffer, pH 8.6, were used. Reactions were initiated by addition of 200 μl of the enzyme preparation. The reaction progress was monitored by withdrawing 0.5-ml samples at 0, 5, and 10 min, using a syringe needle to reduce evaporation of the substrate from the reaction mixture. The samples were mixed with 0.5 ml of methanol to terminate the reaction. The substrate and product concentrations were analyzed on a gas chromatograph equipped with a capillary column (DB-FFAP 30 m × 0.25 mm × 0.25 μm, J&W Scientific) using a flame ionization detector (GC Trace 2000, Finnigan). The temperature program was isothermal at 40 °C for 1 min followed by increase to 250 °C at 20 °C/min. The programmed flow of carrier gas (He) started at 0.6 ml/min for 1 min and then increased to 2.0 ml/min at 0.2 ml/min/min. Michaelis-Menten kinetic constants were calculated from the initial steady-state rates of product formation by nonlinear regression analysis using ORIGIN 6.1 (OriginLab Corporation).

Inhibition Kinetics—Substrate to product conversion by the action of LinB was monitored using an isothermal titration calorimeter type CSC 4200 (Calorimetry Sciences Corporation). Product inhibition was tested by monitoring of the enzymatic reaction in the presence and absence of a fixed amount of corresponding products. For this, substrate was dissolved in glycine buffer and allowed to achieve thermal equilibrium in the reaction cell (1.3 ml). The reaction was initiated by injecting 20 μl of 30 μM LinB solution. The measured rate of heat change is directly proportional to the velocity of enzymatic reaction according to the equation $\delta Q/\delta t = -\Delta H V \delta[S]/\delta t$, where ΔH is the enthalpy of the reaction, [S] is substrate concentration, and V is the volume of the cell. ΔH was determined by titrating the substrate into the reaction cell containing the enzyme. Each reaction was allowed to proceed to completion. The integrated total heat of reactions was divided by the amount of injected substrate. The evaluated rate of substrate depletion ($-\delta[S]/\delta t$), and corresponding substrate concentrations were then fitted by nonlinear regression to kinetic models using the ORIGIN 6.1 (OriginLab Corporation).

PreSteady-State Kinetics—Stopped flow fluorescence measurements of intrinsic protein fluorescence was used to study the kinetics of substrate conversion. The experiments were performed both on stopped flow instrument model SX17MV (Applied Photophysics) and on SFM-20 stopped flow spectrofluorometer (BioLogic) equipped with a Xe arc lamp with excitation at 295 nm. Fluorescence emission from Trp residues was observed through a 320-nm cutoff filter supplied with the instrument. All reactions were performed at 37 °C in a glycine buffer, pH 8.6. The concentrations reported below are those present in the reaction chamber.

Rapid quench flow experiments were performed at 37 °C in a glycine buffer, pH 8.6, using both a rapid quench flow instrument model RQF-63 (KinTek Instruments) and model QFM 400 (BioLogic). Reactions were started by rapid mixing of 50 μl of enzyme with 50 μl of substrate solution. Quenching was done with 120 μl of 0.4 M H_2SO_4 (final concentration) after time intervals ranging from 2 ms to 2 s. The quenched mixture was directly injected into 0.5 ml of ice-cold diethyl ether containing 0.05 mM 1,2-dichloropropane as the internal standard. After extraction, the diethyl ether layer containing non-covalently bound substrate and product was separated from the water phase and neutralized by addition of $NaHCO_3$. The water was eliminated by addition of Na_2SO_4, and the diethylether extract was transferred to an autosampler vial for automated analysis. The samples were analyzed on a gas chromatograph equipped with a flame ionization detector (Hewlett Packard 6890) and a capillary column (HP-5 25 m × 0.25 mm × 0.25 μm, Chrompack). The temperature program was 1 min isothermal at 45 °C followed by an increase to 250 °C at 20 °C/min. The flow of carrier gas (N_2) was constant at 1.3 ml/min. All reported concentrations are in the reaction loop of rapid quench flow instrument.

Derivation of Rates—The fluorescence traces (F) of multiple turnover experiments were fitted to a single exponential of the form $F = A \times \exp(-k_{obs}t) + E$ using the program MICROMATH SCIENTIST 2.0 (ChemSW). The parameter A is the amplitude, k_{obs} is the observed rate constant, and E is the floating end point. Equation 1 or 2 was fitted to the k_{obs} data to obtain the respective kinetic constants. Single turnover stopped flow fluorescence and rapid quench flow data were fit to an appropriate kinetic scheme using GEPASI 3.2 (17). The single turnover data were fitted by numerical simulation using the kinetic constants from multiple turnover and steady-state experiments as starting values. The kinetic constants were refined by comparing fits of the single turnover data and the k_{obs} data. To simulate the experimental fluorescence traces with the obtained kinetic constants and reaction schemes, the traces were described as a sum of the contributions of each enzyme species to the total fluorescence.

Modeling of Protein-Ligand Complexes—Crystal structure coordinates of the LinB enzyme were obtained from Protein Data Bank (PDB ID 1CV2). The polar hydrogens were added to the structure by WHATIF 5.0 (18). The catalytic His-272 was singly protonated in the Nδ on accordance with its catalytic function. The script q.kollua was used for addition of charges on all enzyme atoms and script addsol for addition of solvation parameters to the carbon atoms in the protein structure (19). The complex of LinB with halide bound in the active site cavity was obtained using the superimpose function of the visualizing program INSIGHTII 95 (Accelrys). All rotatable bonds were specified in each of the substrates using the program AUTOTORS of AUTODOCK 3.0 (19). Enzyme(-halide)-substrate complexes were modeled by AUTODOCK 3.0 using the Lamarckian Genetic Algorithm (19). Fifty docking runs were performed for each enzyme(-halide)-substrate complex. Calculated substrate orientations were clustered with a clustering tolerance for the root mean square positional deviation of 0.5 Å, but orientations of 1-chlorohexane and 1-bromohexane in LinB-halide complexes were clustered with a clustering tolerance of 1 Å in order to reduce number of obtained orientations.

RESULTS

Site-directed mutagenesis and structural analysis of LinB suggest that Asp-108, His-272, and Glu-132 comprise the catalytic triad in this enzyme (20, 21). The proposed reaction cycle (see Reaction Scheme I) is initiated by binding of the substrate in the Michaelis complex (E·RX).The binding site for the halogen that is cleaved off is formed by Asn-38, Trp-109, and Pro-208. The binding step is followed by a nucleophilic attack of Asp-108 on the carbon atom to which the halogen is bound, leading to cleavage of the carbon-halogen bond and formation of alkyl-enzyme intermediate (E-R·X^-). The intermediate is subsequently hydrolyzed by activated water, with His-272 acting as a base catalyst, which gives formation of the enzyme-product complex (E·ROH·X^-). The function of Glu-132 is to keep His-272 in the proper orientation and to stabilize the positive charge that develops on histidine imidazole ring during the reaction. The final step is release of the products as shown in Reaction Scheme I.

$$E + RX \underset{k_{-1}}{\overset{k_1}{\rightleftharpoons}} E{\cdot}RX \underset{k_{-2}}{\overset{k_2}{\rightleftharpoons}} E\text{-}R{\cdot}X^- \underset{k_{-3}}{\overset{k_3}{\rightleftharpoons}} E{\cdot}ROH{\cdot}X^- \underset{k_{-4}}{\overset{k_4}{\rightleftharpoons}} E + X^- + ROH$$

REACTION SCHEME I

Four substrates were selected as model compounds for a detailed kinetic study of LinB reaction. Chlorocyclohexane is structurally similar to the natural substrate for LinB 1,3,4,6-tetrachloro-1,4-cyclohexadiene. Bromocyclohexane was selected as a brominated analogue of chlorocyclohexane. Furthermore, 1-chlorohexane was selected as one of the best known substrates for LinB with a $k_{cat}/K_m = 1.6 \times 10^5$ $M^{-1}{\cdot}s^{-1}$, and 1-bromohexane as its brominated analogue. However, 1-bromo-

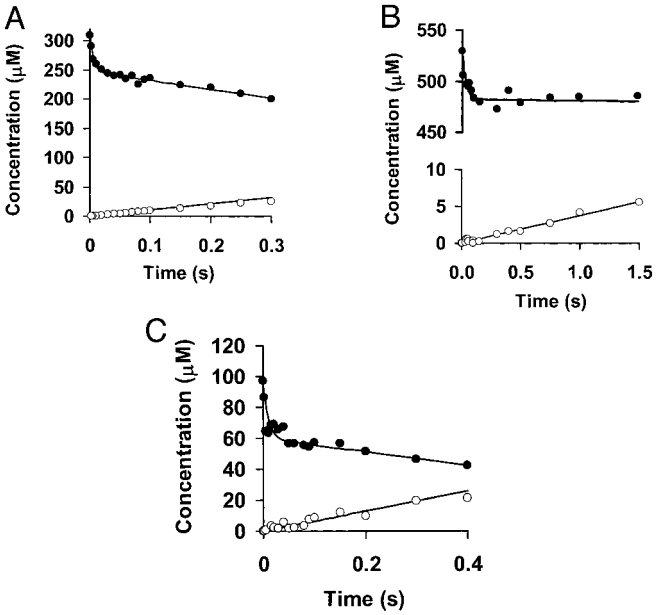

FIG. 1. **Rapid quench flow analysis of burst of LinB reaction.** The burst of the reaction monitored upon mixing of enzyme with substrate to a final concentration of 310 μM bromocyclohexane with 65 μM LinB (*A*), 530 μM chlorocyclohexane with 50 μM LinB (*B*), and 100 μM 1-chlorohexane with 45 μM LinB (*C*) at 37 °C and pH 8.6. Substrate (●) and product (○) concentrations were analyzed by gas chromatography.

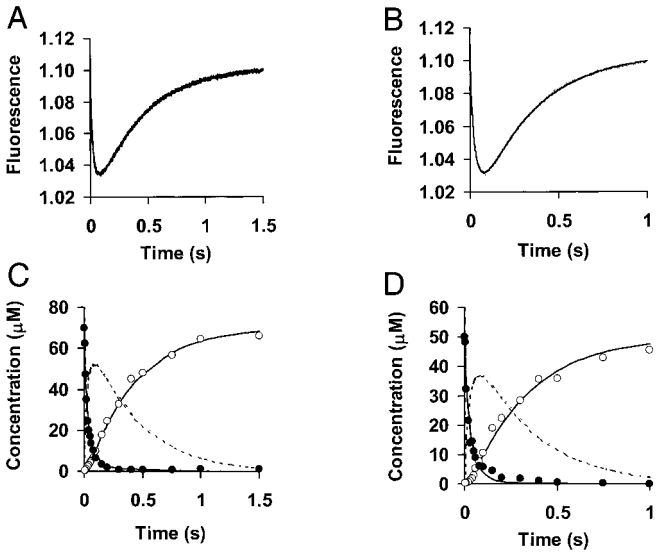

FIG. 2. **Stopped flow fluorescence and rapid quench flow analysis of LinB single turnover.** Fluorescence traces recorded upon rapid mixing of enzyme with substrate to a final concentration of 70 μM bromocyclohexane with 90 μM LinB (*A*) and 40 μM 1-chlorohexane with 80 μM LinB (*B*). Single turnover rapid quench flow data were measured upon mixing of 70 μM bromocyclohexane with 160 μM LinB (*C*) and 50 μM 1-chlorohexane with 160 μM LinB (*D*). Substrate (●) and product (○) concentrations were analyzed by gas chromatography. The *solid line* represents a simulation of the fluorescence signal (*A* and *B*) and the substrate and product concentrations in time (*C* and *D*). The *dashed line* is the simulated concentration of the alkyl-enzyme intermediate. The kinetic parameters from Table I and Reaction Scheme II were used for the simulation.

hexane was later excluded from the set of substrates because its high volatility and low water solubility, which prevented usage of the rapid-mixing instruments for transient kinetic measurement.

Burst of the Reaction—Upon rapid mixing of LinB with excess of substrate, a clear presteady-state burst of substrate depletion was observed while alcohol formation showed no sign of burst for all selected substrates (Fig. 1). The occurrence of the burst of substrate depletion indicates that all the steps before and including cleavage of the carbon-halogen bond (formation of alkyl-enzyme intermediate) are not rate-limiting. The absence of a burst of alcohol formation (hydrolysis of alkyl-enzyme intermediate) suggests that this particular step is the slowest in the catalytic cycle and that all following steps are faster.

Single Turnover Reaction—Single turnover reactions of LinB with bromocyclohexane and 1-chlorohexane were examined to obtain more information about the rates of the separate steps hidden within the observed presteady-state burst of substrate consumption. The single turnover fluorescence traces showed two phases (Fig. 2, *A* and *B*); *i.e.* a fast quenching phase and a subsequent slower recovery of the enzyme fluorescence. A single turnover rapid quench flow experiment was performed to find out which enzyme form caused the fluorescence quenching (Fig. 2, *C* and *D*). The rapid quench flow experiments showed fast disappearance of a substrate and relatively slow formation of a product. Within 200 ms after mixing, almost no substrate was left and less than half of the alcohol was formed, meaning that a covalent intermediate had accumulated. This accumulation of intermediate coincided with the quenching of the fluorescence signal. Thus, the two steps observed in the single turnover experiments represent formation of the alkyl-enzyme intermediate and recovery of free enzyme by hydrolysis of the intermediate. Both for bromocyclohexane and for 1-chlorohexane, the formation of the Michaelis complex appears to be a very fast process, which is not observed as a kinetically distinct phase preceding the formation of alkyl-enzyme intermediate. Single turnover experiments with chlorocyclohexane could not be conducted because of the high K_m of this substrate.

Product Binding and Release—The product inhibition patterns were examined to obtain information about the mechanism of product release. The LinB reaction was assayed in the presence and absence of a fixed amount of the corresponding products using isothermal titration calorimetry. Inhibition of LinB bromocyclohexane hydrolysis by bromide and cyclohexanol (Fig. 3, *A* and *B*) and inhibition of LinB 1-chlorohexane hydrolysis by chloride and 1-hexanol (Fig. 3, *C* and *D*) was examined using Lineweaver-Burk plots. For all products the same intercept was observed, whereas the slopes differed suggesting that the inhibitors had no effect on the initial velocity but only increased the apparent K_m. From these results, the competitive inhibition pattern was deduced for both halide and alcohol inhibition. The kinetics of 1-chlorohexane conversion in the presence of chloride also showed substrate inhibition. The data were further analyzed by fitting the equations for competitive, noncompetitive, and mixed inhibition models. The best fit was evaluated by comparison of S.E. and variance. The halide inhibition data were fitted best with the competitive model, which yielded inhibition constants for chloride (K_i = 888 ± 45 mM) and for bromide (K_i = 282 ± 21 mM.) Also 1-hexanol (K_i = 3.3 ± 0.1 mM) and cyclohexanol (K_i = 43 ± 1.3 mM) were competitive inhibitors of LinB reaction.

Stopped flow fluorescence experiments were used to study kinetics of product binding to LinB. Halide binding showed rapid equilibrium behavior, since the quenching of fluorescence occurred in the dead time of the instrument (1.5 ms). Only steady-state fluorescence levels were observed, suggesting that halide binds to the enzyme active site very quickly (Fig. 4*A*). The dissociation constants calculated from the steady-state fluorescence experiments were K_d = 806 ± 88 mM for chloride and K_d = 471 ± 31 mM for bromide. These values are close to those calculated from halide inhibition data.

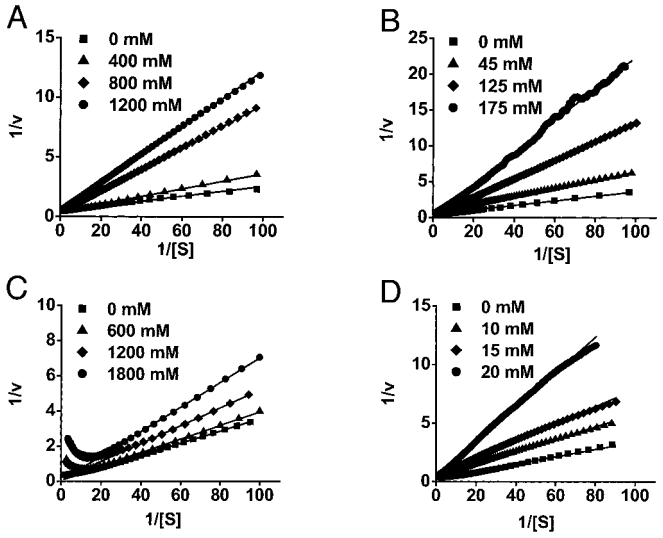

FIG. 3. **Steady-state analysis of product inhibition patterns.** Lineweaver-Burk (1/*v versus* 1/[S]) plots demonstrating the effect of bromide (*A*) and cyclohexanol (*B*) on bromocyclohexane hydrolysis and chloride (*C*) and 1-hexanol (*D*) on 1-chlorohexane hydrolysis catalyzed by LinB.

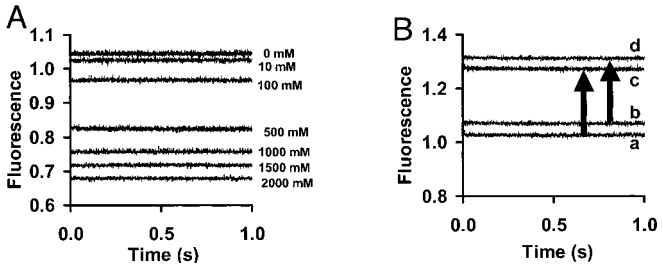

FIG. 4. **Kinetics of halide binding to LinB (*A*) and halide release from LinB (*B*).** *A*, fluorescence traces obtained upon mixing of 10 μM LinB with bromide to a final concentration of 0–2000 mM at 37 °C and pH 8.6. *B*, 20 μM LinB premixed with 600 mM bromide was diluted 1:1 with glycine buffer containing the same concentration of bromide in the absence (*a*) or presence (*b*) of 150 mM cyclohexanol. LinB (20 μM) premixed with 600 mM bromide was diluted 1:1 with pure glycine buffer in the absence (*c*) and presence (*d*) of 150 mM cyclohexanol. The *arrows* show the fluorescence increase observed upon dilution.

The rate of halide release was evaluated in the absence and in the presence of alcohol. For this, LinB was premixed with 600 mM bromide and diluted 1:1 with glycine buffer. An increase of steady-state fluorescence was observed after dilution (Fig. 4*B*). The amplitude of bromide release was not significantly influenced by the presence of the alcohol. This indicates that alcohol and halide do not compete for the same binding site and the release of one product is not dependent on the presence of the other. Together with the finding that both alcohol and halide are competitive inhibitors, this implies a random sequential mechanism for product release.

The amplitude of the fluorescence change that is observed upon mixing of LinB with cyclohexanol and 1-hexanol was not sufficient for a detailed fluorescence evaluation of alcohol binding. Similar to what was found with halide, only steady-state changes of fluorescence could be observed, suggesting that also alcohol binding reaches rapid equilibrium in the dead time of the stopped flow instrument. Considering that the release of both alcohol and halide reach rapid equilibrium and that the enzyme-bound complexes of both products have high dissociation constants, the reaction mechanism from Reaction Scheme I can be simplified to Reaction Scheme II.

Since no products of the reverse reaction have been detected with DhlA (9) or DhaA (14) the dehalogenation reaction can be

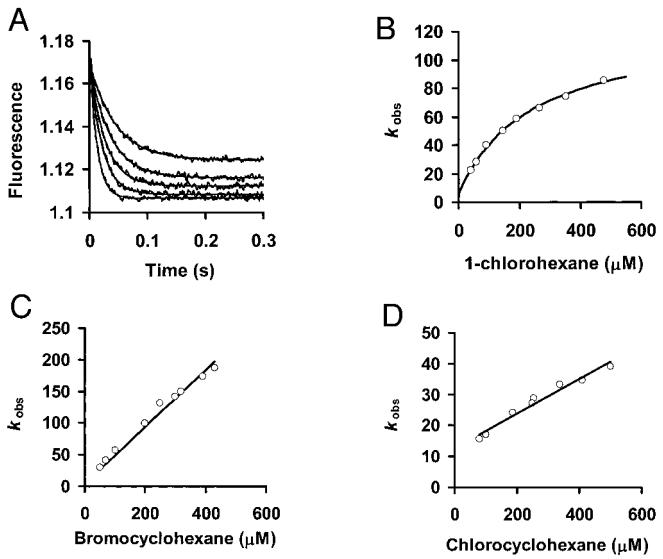

FIG. 5. **Stopped flow fluorescence analysis of LinB multiple turnover.** *A*, fluorescence traces recorded upon rapid mixing of 5 μM enzyme with 40, 60, 90, 150, and 350 μM of 1-chlorohexane at 37 °C and pH 8.6. Each trace shown is the average of 6–10 individual experiments (depending on the signal). The data were fitted with single exponential, yielding a rate constant (k_{obs}) for each concentration. The observed rate constants (k_{obs}) are plotted as a function of 1-chlorohexane (*B*), bromocyclohexane (*C*), and chlorocyclohexane (*D*) concentration. The *solid lines* show the fit of analytical solution (Equation 1 or 2) and the parameters of Table I.

regarded as irreversible. In incubations of LinB (1 μM) with: (i) 65 mM cyclohexanol and 300 mM bromide, (ii) 65 mM cyclohexanol and 800 mM chloride, (iii) 1 M 1-butanol and 1 M chloride, and (iv) 5 mM 3-bromopropan-1-ol and 1 M chloride, respectively, no enzymatic reaction was observed using isothermal titration calorimetry and gas chromatography. These results confirmed that dehalogenation reaction of LinB is also irreversible. Lewandowicz and co-workers (35) and Paneth (36) discussed on the basis of kinetic chlorine isotope effects that the carbon-halogen bond cleavage of 1,2-dichloroethane by DhlA can be reversible, and the hydrolysis of the alkyl-enzyme intermediate is responsible for overall irreversibility of haloalkane dehalogenases reaction. Therefore the cleavage of the carbon-halogen bond was included as a reversible step in Reaction Scheme II.

$$E + RX \underset{}{\overset{K_s}{\rightleftharpoons}} E{\cdot}RX \underset{k_{-2}}{\overset{k_2}{\rightleftharpoons}} E\text{-}R{\cdot}X \xrightarrow{k_3} E + ROH + X^-$$

REACTION SCHEME II

Multiple Turnover Reaction—Since formation of the Michaelis complex appears to be a very fast process, it is best described as a rapid equilibrium with dissociation constant K_s. The analysis of single turnover reactions, using stopped flow and rapid quench flow techniques, did not provide sufficient information to yield a unique solution for the equilibrium constant, and therefore multiple turnover experiments were performed. Multiple turnover reactions with chlorocyclohexane, bromocyclohexane, and 1-chlorohexane were examined using the stopped flow fluorescence technique. The obtained traces were fitted with single exponentials (Fig. 5*A*), yielding an observed rate constant for each substrate concentration (k_{obs}). A relationship between k_{obs} and the microscopic rate constants (Equation 1) was derived using Reaction Scheme II. The dependence of k_{obs} on the 1-chlorohexane concentration showed saturation (Fig. 5*B*). Thus, k_2 and K_s could be determined separately. The dependence of k_{obs} on the bromocyclohexane and chlorocyclo-

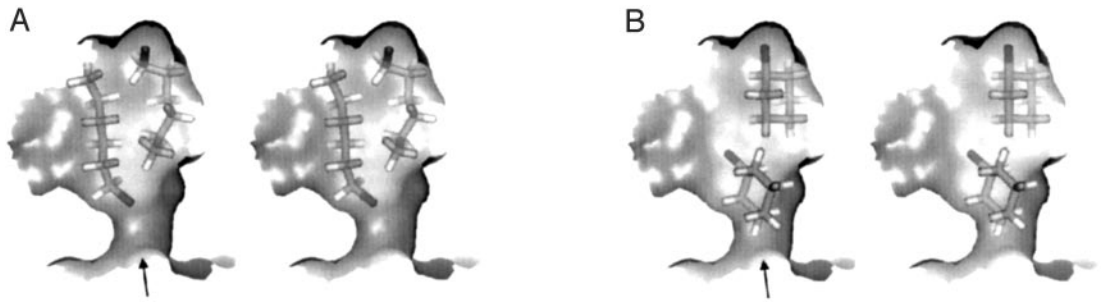

FIG. 6. **Models of the enzyme-substrate complexes.** Complexes of LinB with 1-chlorohexane (*A*) and chlorocyclohexane (*B*) prepared by two consecutive dockings. The enzyme active site is represented by a molecular surface with the entrance tunnel indicated by the *arrow*. The substrate molecules are represented by *sticks*. The results are shown for the chlorinated substrates only because the orientation and position of brominated analogues was comparable.

TABLE I
Kinetic constants of haloalkane dehalogenase LinB determined at 37°C and pH 8.6

Substrate	K_s	k_2	k_2/K_s	k_{-2}	k_3	K_m[a]	k_{cat}[a]	k_{cat}/K_m[a]
	μM	s^{-1}	$\mu M^{-1}\cdot s^{-1}$	s^{-1}	s^{-1}	μM	s^{-1}	$M^{-1}\cdot s^{-1}$
Chlorocyclohexane	>500	>40	0.06 ± 0.01	—[b]	—[b]	221 ± 56	0.1 ± 0.01	5.0×10^2
Bromocyclohexane	>450	>200	0.45 ± 0.02	1.1 ± 0.4	2.5 ± 0.07	23 ± 5	1.8 ± 0.26	7.8×10^4
1-Chlorohexane	240 ± 44	117 ± 5	0.50 ± 0.04	0.4 ± 1.0	3.2 ± 0.19	16 ± 4	2.6 ± 0.27	1.6×10^5

[a] Michaelis-Menten parameters determined under steady-state conditions.
[b] The values could not be derived; $(k_3 + k_{-2}) = 12.5\ s^{-1}$ obtained from the intercept after fitting of Equation 2 to multiple turnover data.

hexane concentrations (Fig. 5, *C* and *D*) showed no saturation behavior even after reaching the limit of substrate solubility. This indicates that the K_s is high, leading to a simplification of the function for k_{obs} (Equation 2). In this case, only the ratio k_2/K_s could be determined and only the lower limits of k_2 and K_s could be obtained for these substrates.

$$k_{obs} = \frac{k_2 \cdot [S]}{[S] + K_s} + k_{-2} + k_3 \qquad \text{(Eq. 1)}$$

$$k_{obs} = \frac{k_2 \cdot [S]}{K_s} + k_{-2} + k_3 \qquad \text{(Eq. 2)}$$

Substrate Inhibition—The kinetics of 1-chlorohexane conversion showed a decrease in velocity at high substrate concentration after the maximum velocity was reached. This is manifested by the upward curvature of the Lineweaver-Burk plot at low values of 1/[S] (Fig. 3*C*) and indicate substrate inhibition. Most often, substrate inhibition is caused by binding of more than one substrate molecule to the active site of an enzyme, resulting in an inactive complex. Substrate inhibition was observed for 1-bromohexane (K_{si} = 0.19 ± 0.09 mM) and 1-chlorohexane (K_{si} = 6450 ± 360 mM). The substrate inhibition constant (K_{si}) for 1-chlorohexane is not significant at standard conditions but becomes relevant in the presence of a high concentration of chloride. This suggests that the $E\cdot(RX)_2$ complex of LinB with 1-chlorohexane has a significant affinity for chloride (K_d = 41 ± 6 mM). The chloride is probably bound in its energetically favorable region in between halide-stabilizing residues, which cannot be reached by any of the competing substrate molecules. Thus the formation of $ES\cdot(RX)_2\cdot X^-$ complex shifts the equilibrium toward inactive enzyme forms and results in enhancement of substrate inhibition effect in the presence of high concentration of halide product. The docking analyses indicated energetically favorable formation of ES_2-halide complex for 1-chlorohexane and 1-bromohexane, while an analogous complex was not observed for chlorocyclohexane and bromocyclohexane.

The structures of LinB complexed with 1-chlorohexane, 1-bromohexane, chlorocyclohexane, and bromocyclohexane were modeled using molecular docking methods. The automated docking procedure provided a suitable orientation of enzyme-substrate complexes (E·RX) for all four selected substrates. The docking of a second substrate molecule into E·RX complexes was further evaluated. Both 1-chlorohexane and 1-bromohexane formed a complex with LinB with two substrates ($E\cdot(RX)_2$) bound abreast deeply in the active site (Fig. 6*A*). It is highly probable that their tight contact prevents both these substrate molecules from positioning itself in such a way that the enzyme can attack. The docking of two cyclic substrate molecules resulted in a complex with the first substrate molecule located in the active site and the second substrate molecule in the entrance tunnel, apparently unable to bind further into active site (Fig. 6*B*). This configuration probably does not prevent the enzyme from reacting with the first substrate molecule.

DISCUSSION

The steady-state as well as presteady-state kinetics of conversion of selected substrates were studied to obtain detailed insights into the catalytic mechanism of the haloalkane dehalogenase LinB. The results led to a proposal of minimal kinetic mechanism consisting of three steps: (i) substrate binding, (ii) cleavage of carbon-halogen bond with simultaneous formation of an alkyl-enzyme intermediate, and (iii) hydrolysis of the alkyl-enzyme intermediate. Import of substrate as well as export of products out of the active site of LinB are fast processes, reaching rapid equilibrium.

The cleavage of the carbon-halogen bond was found to be the fastest step in the catalytic cycle (Table I). The rate of cleavage of carbon-bromide bond is faster than cleavage of carbon-chloride bond, as exemplified from comparison of kinetic constants determined with 1-chlorocyclohexane and 1-bromocyclohexane. This observation is in agreement with bromine being a better leaving group than chlorine in a bimolecular substitution reaction. The same result was found for the substrates 1,2-dichloroethane and 1,2-dibromoethane with the haloalkane dehalogenase DhlA by Schanstra *et al.* (9). The binding of the substrate and the following cleavage of the carbon-halogen bond are fast steps resulting in considerable accumulation of the alkyl-enzyme intermediate. Thus K_m values for LinB are much lower than the K_s values. Accumulation of the intermediate further suggests that the step following the alkylation half-reaction is slow.

Hydrolysis of the alkyl-enzyme intermediate was found to be

TABLE II
Kinetic constants of the haloalkane dehalogenases DhlA, DhaA and LinB

Enzyme	Substrate	K_s	k_2	k_{-2}	k_3	k_4	K_m	k_{cat}	k_{cat}/K_m
		μM	s^{-1}	s^{-1}	s^{-1}	s^{-1}	μM	s^{-1}	$\mu M^{-1} \cdot s^{-1}$
DhlA wt	1,2-Dibromoethane[a]	>27	>130	—	10 ± 2	4 ± 1.5[h]	10	3	0.3
DhlA Val226Ala	1,2-Dibromoethane[b]	110	60 ± 20	—	12 ± 3	43 ± 10[h]	33	8.2	0.25
DhlA Phe172Trp	1,2-Dibromoethane[c]	63	30 ± 5	—	9 ± 1.5	75 ± 25[h]	25	5.9	0.24
DhlA Trp175Tyr	1,2-Dibromoethane[d]	250	70 ± 15	—	8 ± 0.7	16 ± 2[h]	60	5.8	0.0008
DhlA D260N + N148E	1,2-Dibromoethane[e]	700	0.55 ± 0.05	—	0.8 ± 0.1	>10[h]	430	0.35	0.0008
DhlA wt	1,2-Dichloroethane[a]	2222	50 ± 10	—	14 ± 3	8 ± 2[h]	530	3.3	0.0062
DhlA Val226Ala	1,2-Dichloroethane[b]	5555	14 ± 1	—	9 ± 2	50 ± 10[h]	1500	3.8	0.0025
DhlA Phe172Trp	1,2-Dichloroethane[c]	10000	4.5 ± 1	—	9.5 ± 1	>75[h]	5130	2.9	0.0006
DhaA wt	1,3-Dibromopropane[f]	60–300	300 ± 60	—	14.8 ± 0.7	3.9 ± 0.6[i]	5	3.7	0.54
LinB wt	Chlorocyclohexane[g]	>500	>40	—	—	—	221	0.1	0.0005
LinB wt	Bromocyclohexane[g]	>450	>200	1.1 ± 0.4	2.5 ± 0.07	—	23	1.8	0.08
LinB wt	1-Chlorohexane[g]	240	117 ± 5	0.4 ± 1	3.2 ± 0.2	—	16	2.6	0.16

[a] Determined at pH 8.2 and 30°C (9).
[b] Determined at pH 8.2 and 30°C (22).
[c] Determined at pH 8.2 and 30°C (23).
[d] Determined at pH 8.2 and 30°C (24).
[e] Determined at pH 8.2 and 30°C (31).
[f] Determined at pH 9.4 and 30°C (14).
[g] Determined at pH 8.6 and 37°C (this study).
[h] Halide release.
[i] Alcohol release.

the slowest step in the kinetic mechanism of LinB using chlorocyclohexane, bromocyclohexane, and 1-chlorohexane as model substrates. Hydrolysis is therefore the rate-limiting step for the overall kinetics of LinB and it is highly correlated with k_{cat}. It is interesting to note that although dehalogenation of the substrates bromocyclohexane and chlorocyclohexane results in the same alkyl-enzyme intermediate, the rates of their hydrolysis differ significantly, being 33 times slower in the case of chlorocyclohexane. This might be attributed to the presence of a different halide ion in the active site after the first reaction step and its interaction with the transition state structure of the hydrolytic reaction.

Both products are released from the enzyme active site after hydrolysis. Considering the high rate of product release and the high dissociation constants of halide and alcohol from the enzyme the release of products was not included in the kinetic mechanism as a distinct step. Alcohol and halide do not compete for the same binding site, and the release of one product is not dependent on the presence of the other product in the active site of LinB. Taken together with the finding that both an alcohol and a halide are competitive inhibitors for LinB, this implies a random sequential mechanism for the release of products.

A comparison of the kinetic mechanism of LinB with the mechanisms reported for DhlA (8) and DhaA (14) reveals their overall similarity. The binding of the substrate and the cleavage of the carbon-halogen bond are fast steps, resulting in accumulation of the alkyl-enzyme intermediate for all three enzymes (Table II). The main and very important difference in kinetic mechanism is in the rate-limiting step. Whereas the halide release is the predominant rate-limiting step of DhlA (8) and liberation of alcohol is the rate-limiting step of DhaA (14) under steady-state conditions, the release of both halide and alcohol was found to be fast in the catalytic cycle of LinB. The conclusion that there are different rate-limiting steps for three enzymes from the same protein family sharing the same chemical mechanism demonstrates that extrapolation of this important catalytic property of one enzyme to another can be misleading, even for evolutionary closely related proteins. Moreover, site-directed mutagenesis studies of DhlA demonstrated that even a single point mutation may result in the change of the rate-limiting step. Hydrolysis of the alkyl-enzyme intermediate and not a halide release was the slowest reaction step in three single point mutants of DhlA: V226A, F172W, and W175Y (22–24).

The high rate of export of products out of LinB can be explained by the presence of three tunnels connecting the active site with the bulk solvent as well as by the high flexibility of the cap domain (25). Compared with DhlA and DhaA, LinB has a protein core that is more open to the surrounding environment (21) allowing a faster exchange of ligands between the active site and the bulk solvent. Such an exchange was indeed observed for water molecules in a nanosecond molecular dynamics simulation (25). High flexibility of the cap domain, the size and number of the tunnels, and the size of the active site (21) also explain why substrate inhibition was so far reported only for the LinB enzyme. Molecular docking calculations confirmed the ability of LinB to bind even two molecules as large as cyclic and linear halogenated hexanes. DhlA, on the other hand, has a very narrow tunnel and the small active site buried inside the protein core requiring a conformational change for halide solvation and its release from the active site (8).

Another structural difference linked to the export of halide ions from the active site is found in the halide-stabilizing residues (26). One of two primary halide-stabilizing residues (Trp-125 in DhlA, Trp-107 in DhaA, and Trp-109 in LinB) is fully conserved in all haloalkane dehalogenases, while the second residue differs both by its nature and location within the protein structures (Trp-175 in DhlA, Asn-41 in DhaA, and Asn-38 in LinB). The degree of halide stabilization obtained with two tryptophan residues is stronger, as apparent from a comparison of wild-type and mutant enzymes: K_d for binding of chloride to DhlA (9) is 75 mM (pH 8.2, 30 °C); K_d for binding of chloride to LinB is 805 mM (pH 8.6, 37 °C) and K_d for chloride binding to W175Y DhlA (24) is >1000 mM (pH 8.2, 30 °C). Structure-function relationships described above provide an explanation why the site-directed mutagenesis (22–24, 26–30)[1] and directed evolution (32–34) studies resulting in changed catalytic properties of haloalkane dehalogenases targeted primarily the tunnel and the halide-stabilizing residues.

[1] Chaloupkova, R., Sykorova, J., Prokop, Z., Jesenska, A., Monincova, M., Pavlova, M., Nagata, Y., and Damborský, J. (2003) *J. Biol. Chem.*, in press.

REFERENCES

1. Ollis, D. L., Cheah, E., Cygler, M., Dijkstra, B., Frolow, F., Franken, S. M., Harel, M., Remington, S. J., Silman, I., Schrag, J., Sussman, J. L., Verschueren, K. H. G., and Goldman, A. (1992) *Protein Eng.* **5,** 197–211
2. Damborsky, J. (1998) *Pure Appl. Chem.* **70,** 1375–1383
3. Pries, F., Van den Wijngaard, A. J., Bos, R., Pentenga, M., and Janssen, D. B. (1994) *J. Biol. Chem.* **269,** 17490–17494
4. Kmunicek, J., Luengo, S., Gago, F., Ortiz, A. R., Wade, R. C., and Damborsky, J. (2001) *Biochemistry* **40,** 8905–8917
5. Verschueren, K. H. G., Seljee, F., Rozeboom, H. J., Kalk, K. H., and Dijkstra, B. W. (1993) *Nature* **363,** 693–698
6. Pries, F., Kingma, J., Krooshof, G. H., Jeronimus-Stratingh, C. M., Bruins, A. P., and Janssen, D. B. (1995) *J. Biol. Chem.* **270,** 10405–10411
7. Pries, F., Kingma, J., Pentenga, M., Van Pouderoyen, G., Jeronimus-Stratingh, C. M., Bruins, A. P., and Janssen, D. B. (1994) *Biochemistry* **33,** 1242–1247
8. Schanstra, J. P., and Janssen, D. B. (1996) *Biochemistry* **35,** 5624–5632
9. Schanstra, J. P., Kingma, J., and Janssen, D. B. (1996) *J. Biol. Chem.* **271,** 14747–14753
10. Damborsky, J., and Koca, J. (1999) *Protein Eng.* **12,** 989–998
11. Nagata, Y., Miyauchi, K., Damborsky, J., Manova, K., Ansorgova, A., and Takagi, M. (1997) *Appl. Environ. Microbiol.* **63,** 3707–3710
12. Janssen, D. B., Gerritse, J., Brackman, J., Kalk, C., Jager, D., and Witholt, B. (1988) *Eur. J. Biochem.* **171,** 67–92
13. Kulakova, A. N., Larkin, M. J., and Kulakov, L. A. (1997) *Microbiology* **143,** 109–115
14. Bosma, T., Pikkemaat, M. G., Kingma, J., Dijk, J., and Janssen, D. B. (2003) *Biochemistry* **42,** 8047–8053
15. Terada, I., Kwon, S.-T., Miyata, Y., Matsuzawa, H., and Ohta, T. (1990) *J. Biol. Chem.* **265,** 6576–6581
16. Nagata, Y., Hynkova, K., Damborsky, J., and Takagi, M. (1999) *Protein Exp. Purif.* **17,** 299–304
17. Mendes, P. (1993) *Computer Appl. Biosci.* **9,** 563–571
18. Vriend, G. (1990) *J. Mol. Graphics* **8,** 52–56
19. Morris, G. M., Goodsell, D. S., Halliday, R. S., Huey, R., Hart, W. E., Belew, R. K., and Olson, A. J. (1998) *J. Comp. Chem.* **19,** 1639–1662
20. Hynkova, K., Nagata, Y., Takagi, M., and Damborsky, J. (1999) *FEBS Lett.* **446,** 177–181
21. Marek, J., Vevodova, J., Kuta-Smatanova, I., Nagata, Y., Svensson, L. A., Newman, J., Takagi, M., and Damborsky, J. (2000) *Biochemistry* **39,** 14082–14086
22. Schanstra, J. P., Ridder, A., Kingma, J., and Janssen, D. B. (1997) *Protein Eng.* **10,** 53–61
23. Schanstra, J. P., Ridder, I. S., Heimeriks, G. J., Rink, R., Poelarends, G. J., Kalk, K. H., Dijkstra, B. W., and Janssen, D. B. (1996) *Biochemistry* **35,** 13186–13195
24. Krooshof, G. H., Ridder, I. S., Tepper, A. W. J. W., Vos, G. J., Rozeboom, H. J., Kalk, K. H., Dijkstra, B. W., and Janssen, D. B. (1998) *Biochemistry* **37,** 15013–15023
25. Otyepka, M., and Damborsky, J. (2002) *Protein Sci.* **11,** 1206–1217
26. Bohac, M., Nagata, Y., Prokop, Z., Prokop, M., Monincova, M., Koca, J., Tsuda, M., and Damborsky, J. (2002) *Biochemistry* **41,** 14272–14280
27. Kennes, C., Pries, F., Krooshof, G. H., Bokma, E., Kingma, J., and Janssen, D. B. (1995) *Eur. J. Biochem.* **228,** 403–407
28. Schindler, J. F., Naranjo, P. A., Honaberger, D. A., Chang, C.-H., Brainard, J. R., Vanderberg, L. A., and Unkefer, C. J. (1999) *Biochemistry* **38,** 5772–5778
29. Marvanova, S., Nagata, Y., Wimmerova, M., Sykorova, J., Hynkova, K., and Damborsky, J. (2001) *J. Microbiol. Methods* **44,** 149–157
30. Nagata, Y., Prokop, Z., Marvanova, S., Sykorova, J., Monincova, M., Tsuda, M., and Damborsky, J. (2003) *Appl. Environ. Microbiol.* **69,** 2349–2355
31. Krooshof, G. H., Kwant, E. M., Damborsky, J., Koca, J., and Janssen, D. B. (1997) *Biochemistry* **36,** 9571–9580
32. Gray, K. A., Richardson, T. H., Kretz, K., Short, J. M., Bartnek, F., Knowles, R., Kan, L., Swanson, P. E., and Robertson, D. E. (2001) *Adv. Synth. Catalysis* **343,** 607–616
33. Pikkemaat, M. G., and Janssen, D. B. (2002) *Nucleic Acids Res.* **30,** e35
34. Bosma, T., Damborsky, J., Stucki, G., and Janssen, D. B. (2002) *Appl. Environ. Microbiol.* **68,** 3582–3587
35. Lewandowicz, A., Rudzinsky, J., Tronstad, L., Widersten, M., Ryberg, P., Matsson, O., and Paneth, P. (2001) *J. Am. Chem. Soc.* **123,** 4550–4555
36. Paneth, P. (2003) *Acc. Chem. Res.* **36,** 120–126